UWS1 Test Report

This document summarizes the observed behavior and overall test results of the first wall unit, UWS1.

The initial ground motions induced minor hairline cracking on the web's external surface and at the extremities of the flange boundary. Ground Motion (GM) 2, the first series of accelerations applied in both the west-east and north-south directions, led to crack appearance along the wall-foundation interface. Subsequently, the uniaxial ground motion GM5 generated a maximum west-east drift (δ_{WE}) of 1.74%. This level of loading caused flexural cracks to develop within the bottom storey height (i.e., below the slab) at the flange boundary extremities, exacerbating existing cracks at the wall-foundation interface, which were apparent even after the unit came to rest.

The bi-directional ground motions of GM6 induced noticeable torsion, as expected, in combination with flexural actions, likely due to the offset of the shear centre of the wall specimen (Hoult, 2021; Hoult & Almeida, 2024; Hoult & Beyer, 2020). Concrete crushing was observed during GM6 in the corner of the flange-web south-west intersection. During this ground motion, the maximum δ_{WE}, north-south drift (δ_{NS}), and rotation (θ_{max}) were recorded to be 1.65%, 0.65%, and 25.4 mrad, respectively. Some horizontal sliding at the wall-foundation interface was also visually observed on the north flange face (i.e., Flange Two) along the west-east direction, parallel to the flanges.

Further concrete crushing occurred during GM7 in the south flange (i.e., Flange One) boundary end, and at the flange-web intersection in both the north-west and south-west corners. During GM7, the largest recorded in-plane west-east drift, reaching δ_{WE} = 2.71%, was observed. Subsequently, the largest amplitudes of bi-directional accelerations with GM8 caused significant crushing in both flange boundary ends. The large imposed maximum drifts of δ_{WE} = 1.82%, δ_{NS} = 0.76%, and rotation of θ_{max} = 24.7 mrad from GM8 also resulted in noticeable buckling of the longitudinal rebars in the south-east flange boundary end – see Figure 1a. Upon inspection, a larger-than-prescribed spacing between two consecutive confining rebars in the south-east flange (e.g., Flange One) boundary end was observed, facilitating the aforementioned rebar buckling response. In the north-east flange (e.g., Flange Two), however, the tight confining reinforcement led to high compressive strain demands, inducing noticeable local out-of-plane buckling of the flange towards the inside of the core wall – see Figure 1b.

Videos of the test during GM8 confirmed suspicions of exacerbated horizontal sliding at the wall-foundation interface. The preliminary analysis of the Optitrack motion capture system showed a maximum base sliding displacement of 6.7 mm and 7.9 mm during GM7 and GM8, respectively.

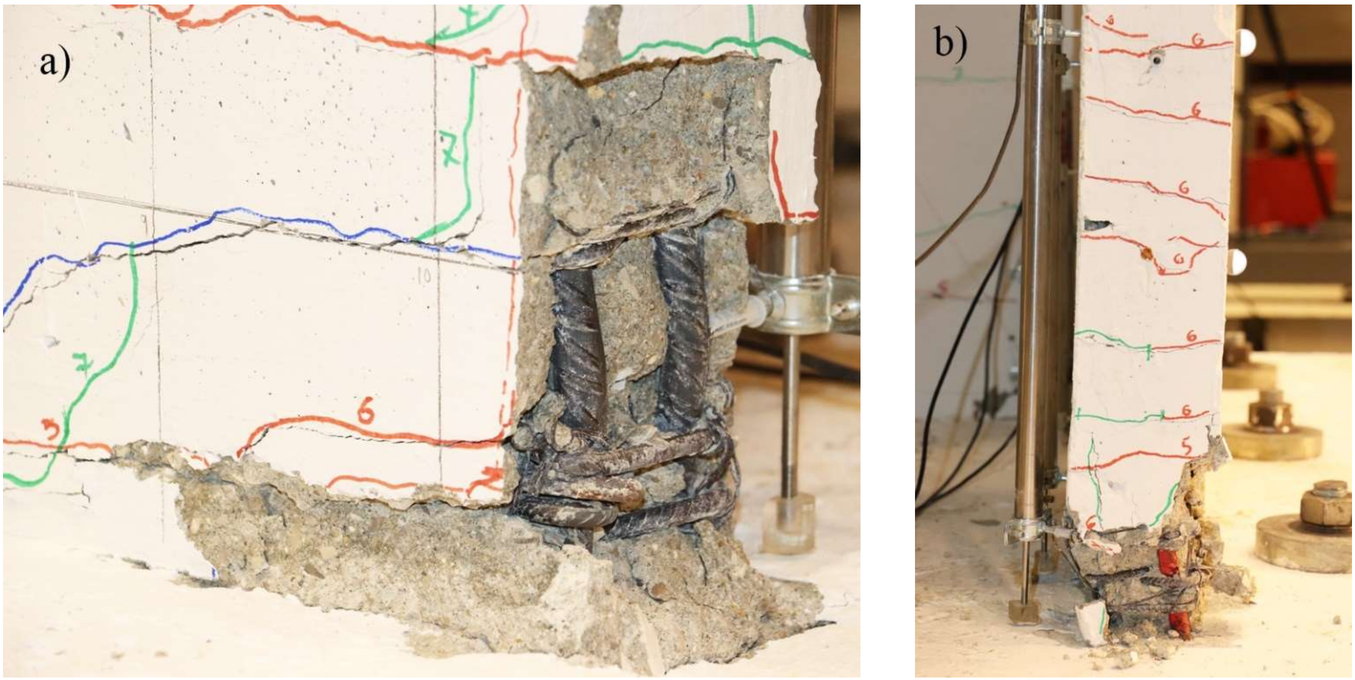

Figure 1 Failure locations of unit UWS1 at the base after GM8 (a) boundary end of Flange One with rebar buckling (b) boundary end of Flange Two with local out-of-plane buckling towards the inside of the wall.

References

Hoult, R. (2021). Torsional capacity of reinforced concrete U-shaped walls. *Structures, 31*, 190-204. doi: https://doi.org/10.1016/j.istruc.2021.01.104

Hoult, R., & Almeida, J. P. d. (2024). Flexure-Torsion Response of Compressed Open Reinforced-Concrete Cores: Experimental Strain Gradients, Numerical Methods, and Interaction Diagrams. *Journal of Structural Engineering*. doi: https://doi.org/10.1061/JSENDH.STENG-13147

Hoult, R., & Beyer, K. (2020). Decay of Torsional Stiffness in RC U-Shaped Walls. *Journal of Structural Engineering, 146*(9). doi: https://doi.org/10.1061/(ASCE)ST.1943-541X.0002733